Peer reviewed version

Link to published version (if available):
10.1117/12.2611744

Link to publication record in Explore Bristol Research
PDF-document

University of Bristol - Explore Bristol Research
General rights

PROCEEDINGS OF SPIE

Design exploration of electro-pneumatic pumps (EPPs) to obtain high pressure and air flow rate improvement

Richard Suphapol Diteesawat, Nahian Rahman, Sam Hoh, Jonathan Rossiter

SPIE.

Design exploration of Electro-pneumatic Pumps (EPPs) to obtain high pressure and air flow rate improvement

Richard Suphapol Diteesawat[1], Nahian Rahman[1], Sam Hoh[1], and Jonathan Rossiter[1]

[1]Department of Engineering Mathematics, University of Bristol, and Bristol Robotics Laboratory, Bristol, UK

ABSTRACT

The Electro-pneumatic Pump (EPP) is a lightweight, flexible electrostatic pump that uses a dielectric-liquid-amplified zipping mechanism to control air volume and pressure and generate high air flow rate. In previous studies, the EPP, made of rectangular insulated electrodes, was capable of inflating/deflating pneumatic actuators and operating as a low power soft pump. This article explores a range of designs for the EPP electrodes to increase pressure generation, air transference and flow rate. As a result, the new EPP was able to generate a maximum pressure of 12.24 kPa, or a pressure difference of 11.25 kPa, corresponding to 481% improvement from the previous study. Additional liquid dielectric at 18% of the maximum available volume enabled the EPP to attain maximum EPP performance. The new design of the EPP was developed by combining two identical zipping regions and minimising the inactive region. Different actuator dimensions and actuation frequencies were investigated. The pump was capable of delivering a maximum flow rate of 238 ml/min at atmospheric pressure (48% improvement) at low power consumption of 0.4 Watt, and it could operate up to 4.47 kPa. It was found that the shape of the zipping region and the behaviour of the integrated compliant spring significantly influences the performance of the device. Lastly, approaches to further improve the EPP pump are discussed.

Keywords: electrically-driven actuator, electrostatic, dielectrophoretic liquid zipping, dielectric liquid, pneumatic, pump

1. INTRODUCTION

Electrically-driven actuators have received growing focus in recent decades due to their fast actuation response and low power consumption.[1,2] These include electroactive polymers (EAPs),[3] dielectric elastomer actuators (DEAs)[4] and electroadhesive actuators.[5] These novel electro-actuators are recognised as one of the highest potential technologies for many robotic fields, including manipulators, locomotion robots, medical applications and wearable assistive devices. One interesting application is to use these technologies to create novel electrically-driven transducers, such as piezoelectric micropumps,[6] zipping dielectric elastomer actuators,[7] and dielectric-liquid-amplified zipping actuators, such as electro-ribbon actuators and HASEL actuators.[8–10] The addition of dielectric liquid has been proved to significantly increase the electrostatic force generation between two insulated electrodes. Consequently, liquid-dielectric-amplified elastomer pumps were developed, including a stretchable fluidic pump (maximum pressure = 14 kPa, maximum averaged flow rate = 6 ml/min),[11] and a circular electrostatic bellow muscle for pneumatic applications (6 kPa, 0.63 l/min).[12] In addition, dry electrostatic pumps using DEAs were developed, including a magnetically-driven dielectric elastomer pneumatic pump (3 kPa, peak flow rate = 0.9 l/min)[13] and a soft dielectric elastomer peristaltic pump (DEPP) for fluidic pumping (4 kPa, peak flow rate = 2.5 l/min).[14]

In practice, only a tiny amount of liquid dielectric is required to achieve high actuation performance due to the benefit of the dielectrophoretic force. A new class of lightweight actuator exploiting this principle have been developed, called Dielectrophoretic Liquid Zipping (DLZ) actuators.[8] The Electro-pneumatic Pump was developed using the DLZ concept, creating a hybrid liquid-pneumatic system that operates as an air-transferring device and a soft pneumatic pump.[15] In previous studies, the EPP could generate pressure up to 2.34 kPa

---

Further author information: (Send correspondence to RSD or JR)
RSD: E-mail: richard.diteesawat@bristol.ac.uk, JR: E-mail: jonathan.rossiter@bristol.ac.uk

and a maximum flow rate of 161 ml/min, operating at low power consumption of 0.5 watts. It can be used to inflate/deflate pneumatic contractile actuators to deliver high contraction at high actuation velocity (32.4% contraction at a speed of 54.4 %/s). In this article, we improve the performance of the EPP by exploring different geometries and designs of the electrodes to increase pressure and flow rate generation. The previous EPP design activated very small electrode zipping areas at high-frequency actuation to deliver high air flow rate, suggesting the potential of smaller EPP designs to produce high flow rate. Therefore, in this work we seek to improve the performance of the EPP by reducing its size, minimising the inactive area, and combining multiple modules in parallel. Thus, a new pump design is introduced with improved pressure and flow rate generation.

2. MATERIAL AND METHOD

2.1 Actuation Concept and Fabrication

The Electro-pneumatic Pump (EPP) is a lightweight, flexible electrostatic pump that encapsulates an electrostatic zipping mechanism inside a flexible pouch to control its internal air volume and to generate pressure and/or air flow (Fig. 1).[15] The EPP exploits the concept of Dielectrophoretic Liquid Zipping (DLZ), which uses liquid dielectric to considerably amplify an electrostatic attractive force and electric field induced between two insulated electrodes when they are electrically charged, thus causing a fast, effective zipping action.[8] The electrostatic force follows Maxwell pressure, $P \propto \varepsilon E^2$, where ε and E are the dielectric permittivity and the electric field, respectively.[16] The addition of dielectric liquid improves both permittivity (ε) and electrical breakdown strength, increasing electric field and electrostatic force by $\left(\frac{E_{breakdown,liquid}^2}{E_{breakdown,air}^2}\right)$. Thanks to the effect of dielectrophoretic forces,[17] only a tiny amount of liquid dielectric is required, which is kept at the zipping point(s), the region of the highest electric field. Fig. 1 demonstrates the actuation of the EPP to inflate a connected pneumatic device. At no actuation, the EPP contains air volume inside its chamber. When applying voltage across two opposite electrodes, an induced electrostatic attractive force causes a progressive zipping motion from zipping edge(s), resulting in air transferring to the connected pneumatic device and an increase in the internal pressure.
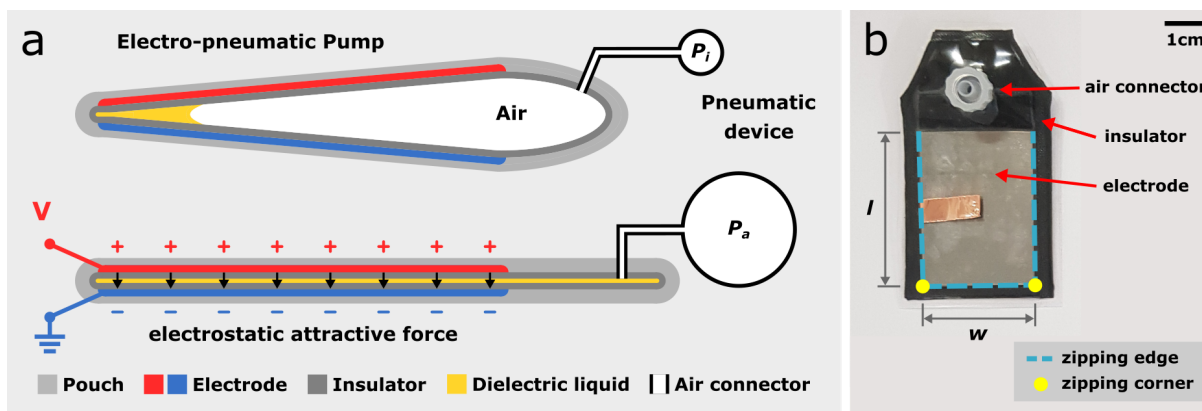

Figure 1: (a) Schematic diagram of the Electro-pneumatic Pump in no actuation and actuation states, demonstrating an electrostatic zipping mechanism with the application of Dielectrophoretic Liquid Zipping (DLZ). (b) A photograph of the fabricated EPP.

The EPP can be simply made of low-cost materials and is customisable and scalable, offering numerous design possibilities. It is fabricated by creating two identical zipping parts and heat sealing them together to form the actuator. Each of them contains three main components: an insulated sheet, a conductive electrode, and a flexible pouch sheet. A 130 μm thickness Polyvinyl chloride (PVC) tape (AT7, Advance Tapes, UK) and a flexible, 125 μm thickness low-density polyethylene (LDPE) sheet (Polybags, UK) were used as the insulation and pouch layers of each identical part. A 0.1 mm thickness thin steel sheet (1.1274 carbon steel, h+s präzisionsfolien GmbH, Germany) was used as an electrode on both parts; its stiffness and flexibility constrained the shape of the zipping mechanism of the EPPs. An additional double-sided adhesive tape (tesa 64621, Germany) was inserted

between the electrode and the pouch to ensure firm adhesion between the electrode and pouch layer. Finally, a small volume of 5-cSt silicone oil (317667, Sigma-Aldrich, USA) was added to the sealed pouch as dielectric liquid to complete the EPP fabrication (density = 0.913 g/ml at 25 °C). The insulated PVC tape and silicone oil have relative permittivities of 4.62 and 2.7 and electrical breakdown voltages of approximately 60 MV/m and 20 MV/m, respectively.

2.2 Experiment Setup and Procedure

Two types of experiments were conducted to evaluate pressure and air flow rate generation (Fig. 2). To improve pressure generation of the EPP, three investigations were performed by varying the dimension of the rectangular electrodes: an electrode width (w), an electrode thickness (t), and an electrode length (l). A tiny volume of dielectric liquid (< 1.0 g or 1.1 ml) was added to all EPPs prior to their experiments. The EPP was directly connected to a pressure sensor (HSCDANN030PGAA5, Honeywell, USA) to measure generated pressure and a syringe to control air volume contained inside the EPP for experiments (Fig. 2a). The injected air volume (v_{in}) from the syringe refers to atmospheric air added to this closed pneumatic system. Note that this does not reflect the actual air volume in the system since air is compressible. The experiment started with a flat EPP as its natural shape, defined as zero injected air volume inside the EPP ($v_{in} = 0$), and its pressure at no actuation is defined as initial pressure ($P_{initial}$ or P_i). Consequently, two electrodes were oppositely charged at a selected voltage (V) by a high voltage amplifier (5HVA24-BP1, UltraVolt, USA) to perform zipping and compress internal air, generating pressure, which was recorded as actuated pressure ($P_{actuated}$ or P_a). The v_{in} was incrementally increased by the syringe from 0 ml to 5 ml to evaluate pressure generation at different v_{in}.
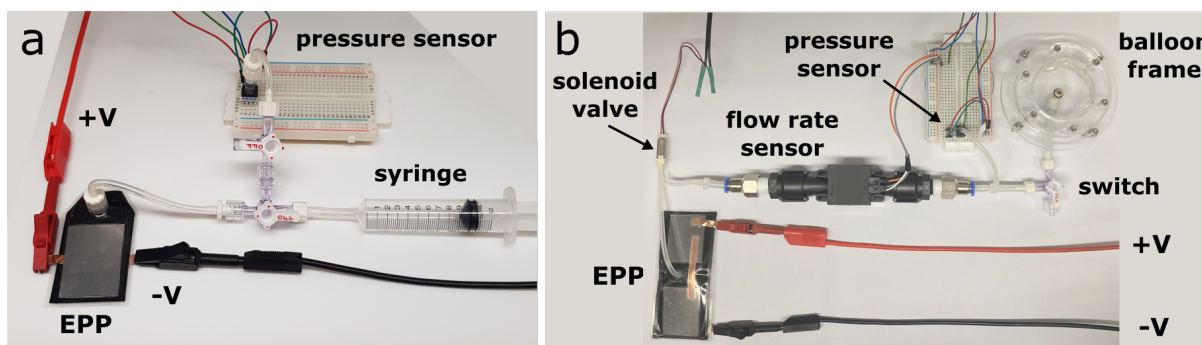

Figure 2: EPP experiments to evaluate (a) pressure generation and (b) air flow rate generation.

The experiment to evaluate air flow rate generation was set as shown in Fig. 2b, where EPPs were connected to a solenoid valve (S070C-RAG-32, SMC, Japan), an air flow rate sensor (AWM510VN, Mass Air Flow Sensor, Honeywell, USA), and the same pressure sensor in sequence. Since the EPPs operate at low pressure, the solenoid valve was selected to measure flow rate instead of using a check valve, which typically requires a minimum cracking pressure (approx. 5 kPa), and to obtain the most accurate evaluation of the EPP performance. The valve was switched on and off in phase with the applied voltage in order to connect EPPs to the flow rate sensor (switch on) or atmosphere (switch off). Hence, an averaged flow rate value can be obtained by averaging the flow rate only during voltage-on period and dividing by two for an entire actuation cycle. The EPP was actuated at incremental frequencies to investigate the change in air flow rate. An additional manual switch was added to the end of the flow rate sensor and pressure sensor to connect to either atmosphere (the end opens to air) or an elastic balloon. This balloon is made of an acrylic foam tape (VHB Tape 4915, 3M, UK), and it expands with increasing pressure. All data were recorded by a data acquisition device (USB-6211, National Instruments, USA), and all experiments were operated through the MATLAB computing program.

3. RESULTS

3.1 Pressure Generation

The EPP is naturally flat when no air volume has been injected. It therefore requires a certain air volume to increase the space between the electrodes and to enable its zipping actuation. Only then will the EPP generate

air pressure when the zipping mechanism is activated. For example, a small 4.4 g EPP made of 3 cm wide, 4 cm long and 0.1 mm thick electrodes was actuated at 8 kV when it contained injected air volume (v_{in}) of 0.8 ml. After electrically charging, the electrodes zipped together, compressing internal air and thus increasing internal pressure. Fig. 3a shows the initial pressure at no actuation (P_i), maximum actuated pressure ($P_{a,max}$) and converged actuated pressure ($P_{a,converged}$) of this EPP when actuated for 10 seconds. This EPP was further actuated at different v_{in}; its pressure generation is illustrated in Fig. 3b. When actuated, the EPP was able to fully zip at low v_{in} with increasing v_{in}, causing the EPP to produce higher P_a as the EPP still performed full zipping. This behaviour remained until it reached maximum pressure generation at certain v_{in} (0.8 ml for this actuator). Increasing v_{in} further prevented the EPP from achieving full zipping and consequently decreased P_a and generated pressure difference (ΔP: $P_{a,max}$ - P_i) until no zipping occurred (around $v_{in} = 5$ ml, where $\Delta P \simeq 0$). The highest $P_{a,max}$ from three trials was 12.24 kPa (an average of 11.87 kPa from Fig. 3b.), corresponding to ΔP of 11.25 kPa ($P_i = 0.99$ kPa) at $v_{in} = 0.8$ ml.
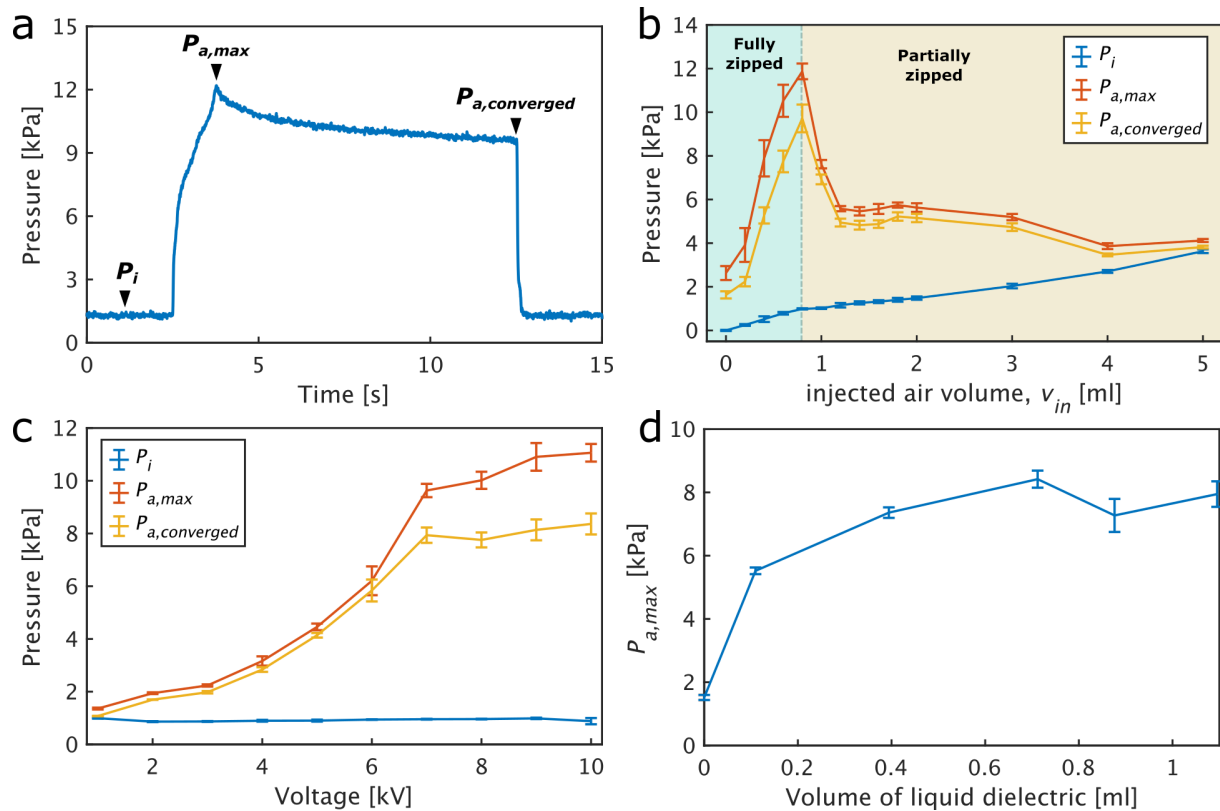

Figure 3: (a) Pressure generation of the EPP ($w = 3$ cm, $l = 4$ cm, and $t = 0.1$ mm). (b) Relationship between v_{in} and pressure generation: initial pressure (P_i), maximum actuated pressure ($P_{a,max}$), and converged actuated pressure ($P_{a,converged}$). (c) Increase in pressure due to increasing voltage. (d) The effect of dielectric liquid on pressure-generating performance at $v_{in} = 0.4$ ml. For (a,b,c) the EPP contained an injected air volume (v_{in}) of 0.8 ml; for (a,b,d) the EPP was actuated at 8 kV.

The effect of different applied voltages was studied and demonstrated in Fig. 3c. $P_{a,max}$ and $P_{a,converged}$ showed a trend of increasing exponentially with increasing voltage, following the theoretical concept of DLZ actuation, where $P \propto V^2$.[8] For this specific $v_{in} = 0.8$ ml, the actuator can fully zip at 7 kV and higher. Fig. 3d illustrates significant improvement in pressure generation due to the addition of liquid dielectric. The EPP generated pressure up to 7.36 kPa with 0.4 ml of liquid dielectric, where the maximum pressure of 7.89 kPa was achieved at the same $v_{in} = 0.4$ ml (Fig. 3b). This proves that 93% of pressure generation can be delivered when the EPP contained liquid dielectric at only 10% of the maximum available EPP volume (4.0 ml). Maximum pressure was reached with liquid dielectric of 0.7 ml or 18% of maximum available volume.

To obtain higher pressure, EPPs made of different electrode dimensions were investigated; they all contained less than 1 g (< 1.1 ml) of liquid dielectric . Fig. 4a illustrates the effect of varying electrode width (w), comparing pressure generation between EPPs made of three different $w = 3$, 4, and 5 cm but with fixed electrode length (l) of 4 cm and fixed electrode thickness (t) of 0.1 mm, at 8kV actuation. The EPP made of smaller w produced higher P_i with increasing v_{in}, reflecting higher constraints in the actuator shape and expansion, and generated higher $P_{a,max}$ but at lower v_{in}. For example, 11.87 kPa at 0.8 ml, 9.47 kPa at 1.2 ml and 5.50 kPa at 2.8 ml for the EPP made of $w = 3$, 4, and 5 cm, respectively (Fig. 4c). Different zipping behaviours were observed in EPPs with different w (Fig. 4d). The EPP with shorter w (3 cm) performed parallel zipping motion toward the opened end (the air connection), whereas the EPP with larger w (5 cm) tended to perform diagonal zipping from both zipping corners. These diagonal zipping motions from left and right corners acted to push against each other, preventing the EPP from deforming effectively and limiting pressure generation (large plateau between 1 ml and 2.8 ml for $w = 5$ cm). This behaviour also appeared in the previous study.[15]
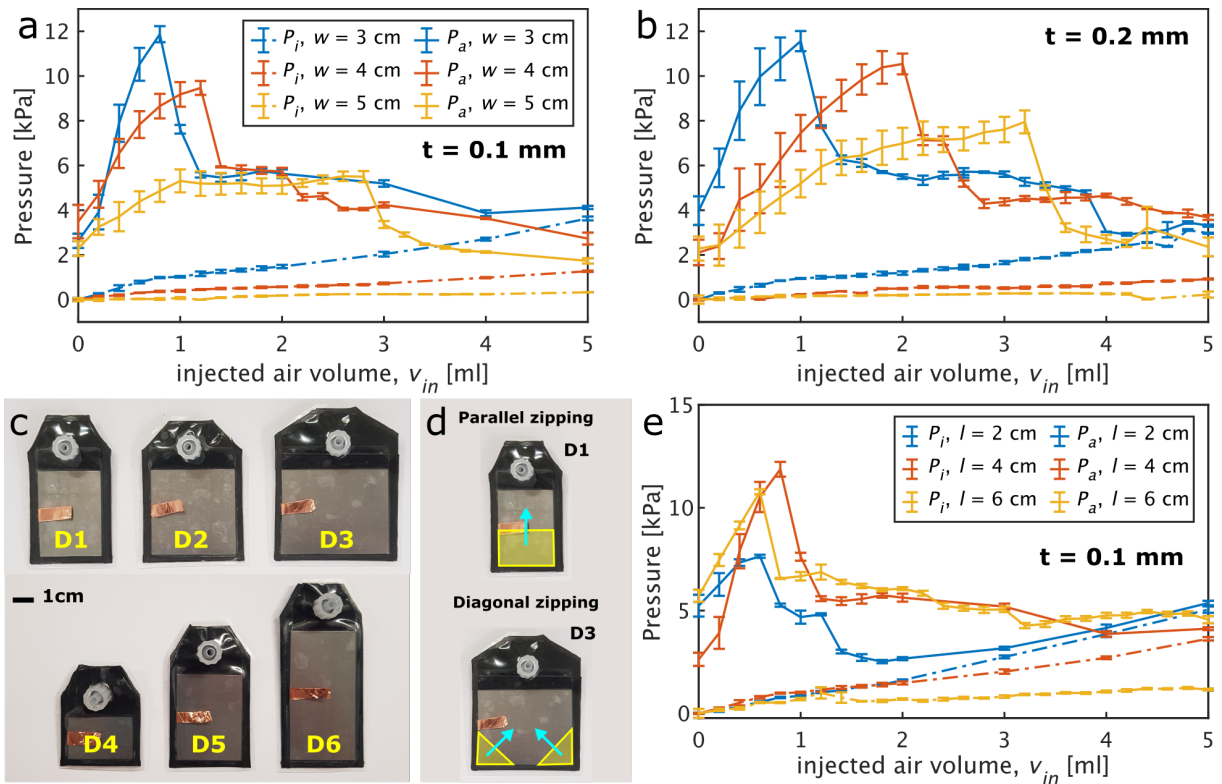

Figure 4: (a-b) Comparison of pressure generation with increasing injected air volume (v_{in}) of the EPPs made of three different electrode widths (w) and the same electrode length ($l = 4$ cm) and the same thickness (t): (a) $t = 0.1$ mm and (b) $t = 0.2$ mm. Both vary w at 3, 4 and 5 cm; P_i and $P_{a,max}$ are presented as dashed-dotted lines and solid lines, respectively. (c) The photograph of tested EPPs when varying w (D1-D3) or l (D4-D6). (d) Schematic diagram showing different zipping behaviour of the EPPs: parallel zipping of the EPPs with small w and diagonal zipping of the EPPs with large w. (e) The effect of varying electrode length on the EPPs made of the same $w = 3$ cm and $t = 0.1$ mm. (a-d) All EPPs were actuated at 8 kV.

Three further EPPs were fabricated with three different electrode widths ($w = 3$, 4 and 5 cm) and the same 4 cm electrode length but thicker electrode ($t = 0.2$ mm) to evaluate the effect of electrode thickness (Fig. 4b). Overall, increasing electrode thickness increased the restoring force of the structure (defined by the material bending stiffness) and reduced the unwanted diagonal zipping behaviour. This increased both pressure generation and the injected air volume (v_{in}) at which the EPPs delivered their $P_{a,max}$. Most notable improvements were seen in EPPs made of $w = 4$ and 5 cm, compared with the finding from Fig. 4a. The $P_{a,max}$ of the EPPs with w

= 3, 4 and 5 cm and $t = 0.2$ mm were 11.56 kPa at $v_{in} = 1.0$ ml, 10.54 kPa at $v_{in} = 2.0$ ml and 7.95 kPa at $v_{in} = 3.2$ ml, respectively (Fig. 4b). Lastly, the effect of electrode length (l) is presented in Fig. 4e, where w and t of all EPPs were fixed at 3 cm and 0.1 mm, respectively, and $l = 2$, 4 and 6 cm. P_i decreased with increasing l but they all had similar P_i at low v_{in} (< 1ml), where $P_{a,max}$ occurred. However, the EPP made of $l = 4$ cm produced the highest $P_{a,max}$, followed by those made of $l = 6$ cm and 2 cm, respectively.

3.2 Air Flow Rate

A new EPP pump design was built by integrating two EPPs together side-by-side and minimising the inactivated regions to improve the air flow rate (Fig. 5). This new EPP contains two identical zipping mechanisms at the left and right ends, and they share the centre area for air connection and as the location of a soft member (foam), used to form an opened zipping mechanism. This allows the actuator to contain more air volume. When activated, the zipping motions move in parallel from the two ends to the centre, compressing and transferring internal air. When deactivated, the foams act as a soft spring, providing a restoring force to return the EPP back to its initial shape. In general, the EPP requires an additional check valve or solenoid valve to enable continuous air pumping to connected devices.
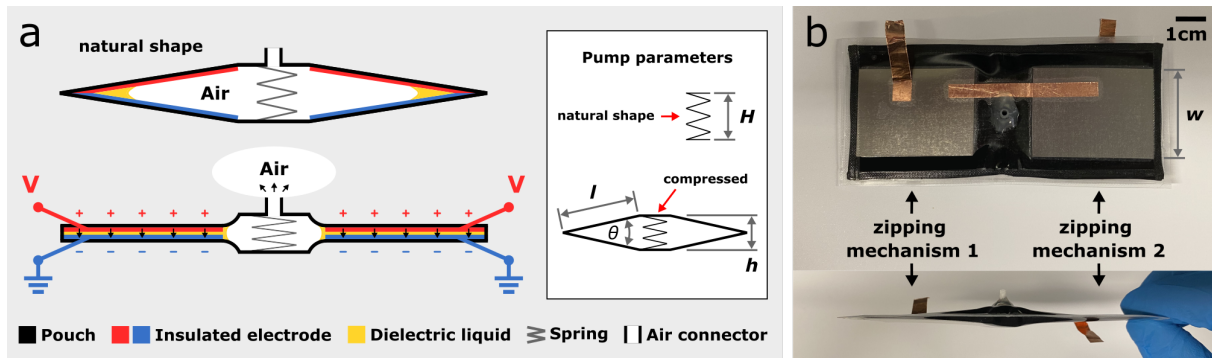

Figure 5: (a) Schematic diagram of the EPP pump, combining two identical zipping halves to minimise an inactive region. (b) Top and side views of the fabricated EPP pump.

Design	Dimension					Weight		$P_{a,max}$ [kPa]
	w [cm]	l [cm]	H [cm]	h [cm]	θ [degree]	Actuator [g]	Liquid dielectric [g]	
1	3	3	0.80	0.54	10.33	6.4	1.1	3.89 ± 0.33
2	3	3	1.0	0.70	13.40	6.5	1.1	2.61 ± 0.15
3	3	4	1.0	0.68	9.75	8.2	1.2	3.77 ± 0.77
4	3	4	1.5	0.75	10.76	8.3	1.4	2.70 ± 0.19
5	4	3	1.0	0.76	14.55	8.5	1.2	2.69 ± 0.12
6	4	3	1.5	0.95	18.22	8.7	1.3	1.15 ± 0.38
7	4	4	1.0	0.71	10.18	10.5	1.5	3.98 ± 0.45

Table 1: The dimension, the weight of the actuator and additional liquid dielectric, and the averaged maximum actuated pressure ($P_{a,max}$) of different EPP pumps at 10kV actuation (average value ± one standard deviation). All pumps made of 0.1-mm thick electrodes.

A range of EPP pumps made of different electrode width (w), electrode length (l) and foam height (H) were built and investigated (Fig. 5). Since the foams are flexible, the fabricated EPP pumps compress them, resulting in a smaller height of the pump (h) (Fig. 5a). The details of the tested pumps are presented in Table 1. Assuming the shape of EPP pumps as shown in the inset of Fig. 5a, where both zipping regions are triangle

in section and the centre region is rectangular, the initial zipping angle at no actuation (θ) can be derived from l and h; therefore, $\theta = 2 \cdot sin^{-1}\left(\frac{h}{2l}\right)$. Hence, for the same electrode dimension (w, l and t), h mainly affects zipping angle θ. First, the EPP pumps (shown in Table 1) were tested to measure their maximum pressure generation by connecting them directly to the pressure sensor for three trials. Since the naturally-expanded shape of these two-sided EPP pumps contain some air, no injected air volume was added to the pump. In this highly constrained test configuration, the pumps only partially zipped until an internal pressure balance was reached. However, when used at lower pressures and larger circuit volumes, the pumps were able to fully zip. EPP pumps with smaller zipping angle (θ) generated higher pressure, $P_{a,max}$ (table 1). For example, pump designs 3 and 7 produced the highest $P_{a,max}$ of 4.59 kPa and 4.47 kPa, respectively.
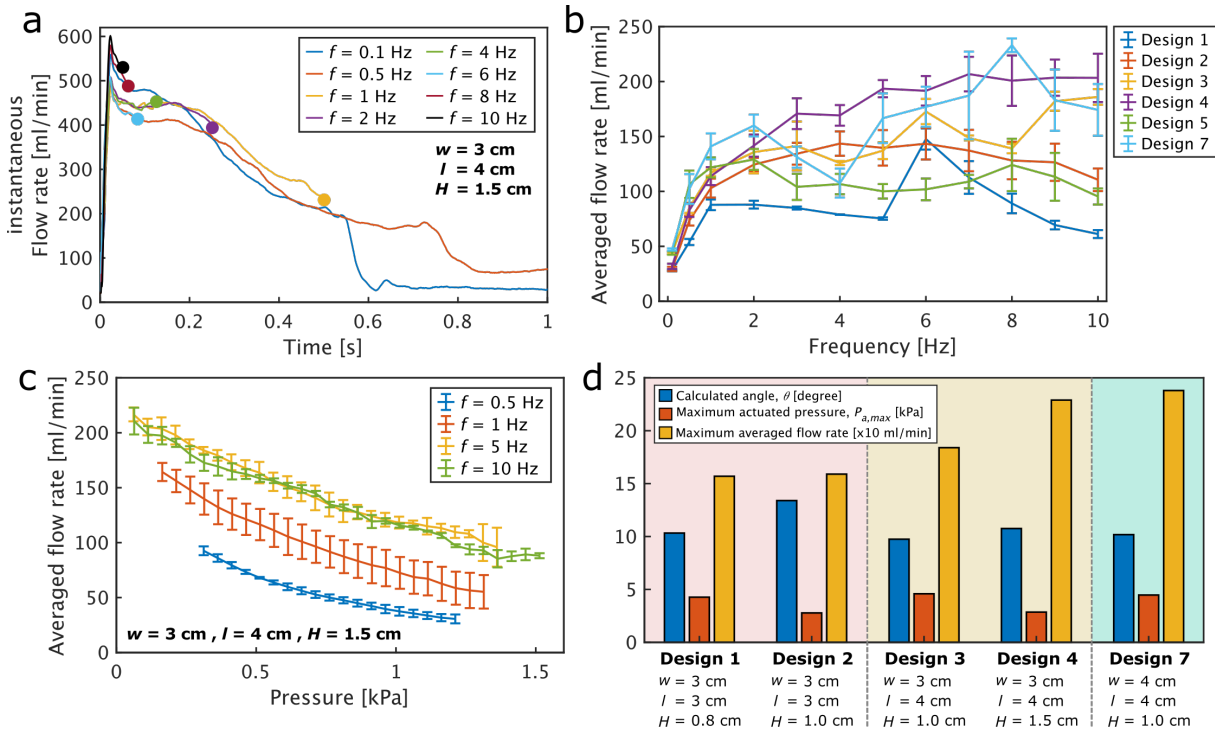

Figure 6: (a) Real-time measured flow rate of the EPP pump design 4 ($w = 3$ cm, $l = 4$ cm, $H = 1.5$ cm) at different frequencies f and at atmospheric pressure (0 kPa); showing only the voltage-on period of a single actuation cycle. Coloured dots specify the last flow rate data during voltage-on period. (b) Averaged flow rate at atmospheric pressure of different pump designs. (c) Averaged flow rate with an increasing back pressure of the pump design 4 at different frequencies. (d) The bar graph showing calculated initial zipping angle (θ), maximum actuated pressure ($P_{a,max}$) and maximum averaged flow rate at atmospheric pressure (the actual values are 10 times the plotted values; x10 [ml/min]) as blue, red and orange bars, respectively. Coloured backgrounds highlight the EPPs made of the same electrode size (w and l). (a-d) All pumps were actuated at 10 kV.

These pumps were further tested to assess their flow rate using the experimental setup shown in Fig. 2b for either (1) maximum flow rate at atmospheric pressure or (2) flow rate at increasing back pressure into the balloon. At atmospheric pressure (0 kPa), the pumps were actuated at different frequencies and periods: 0.1 Hz for 30 seconds and 0.5 - 10 Hz for 10 seconds. The real-time flow rate of the pump design 4 ($w = 3$ cm, $l = 4$ cm, $H = 1.5$ cm) at atmospheric pressure is illustrated in Fig. 6a. Its instantaneous flow rate across different frequencies show similar trend, reaching the peak around 600 ml/min and dropping with time. This shows potential to generate higher flow rate at higher frequency. Fig. 6b demonstrates the averaged flow rate throughout the entire actuation of different pumps at atmospheric pressure. Pump design 7 ($w = 4$ cm, $l = 4$ cm, $H = 1.0$ cm) delivered the highest averaged flow rate of 238 ml/min at 8 Hz actuation. However, the pump design 4 showed better flow-rate trend with increasing frequency, and delivered the highest averaged flow rate

of 229 ml/min at 10 Hz actuation. The soft foam, acting as a soft spring exerting a restoring force, was another factor influencing the flow-rate-generating performance. For example, although the pump design 1 ($w = 3$ cm, $l = 3$ cm, $H = 0.8$ cm) has small zipping angle θ at 10.33 degrees and produced higher pressure, its small foam provides only a small restoring force to return the zipping mechanism back to its original shape within a short period. Thus, the pump always remained partially zipped and produced lower flow rate.

Fig. 6c illustrates the averaged flow rate of the pump design 4 actuated at different frequencies of 0.5, 1, 5 and 10 Hz with increasing pressure using a balloon setup (Fig. 2b). When comparing the maximum pressure and maximum flow rate generation of all pumps, their zipping angle (θ) is a significant factor affecting actuator performance (Fig. 6d). The pump with smaller θ produced higher pressure but lower flow rate, while the pump with larger θ produced less pressure but more flow rate, as seen when comparing between the pump designs 1 and 2 or designs 3 and 4. In addition, when comparing the designs 1, 3 and 7, which have similar θ ($\simeq 10$ degree), they all generated similar maximum pressures (4.27, 4.59 and 4.47 kPa), but a larger pump (larger electrodes) delivered higher flow rate (157, 184 and 238 ml/min, respectively). Lastly, power consumption decreased with increasing frequencies due to a reduction in zipped area. For example, the power consumption of the pump design 4 was 0.40 ± 0.02 Watt (mean $\pm$ one standard deviation) at 0.1 Hz (performed full zipping) and 0.26 ± 0.01 Watt at 10 Hz (partial zipping). Besides, the power consumption of the pump designs 1 and 7 at 10 Hz were 0.18 and 0.38 Watt, respectively, where larger electrodes consumed higher power.

4. CONCLUSION

In this article, we explored alternative designs of the Electro-pneumatic Pump to obtain better performance in terms of pressure and flow rate generation. The effect of varying electrode width (w), length (l) and thickness (t) were studied to achieve higher pressure, and a new design of the EPP pump achieving higher flow rate was introduced. In general, the air volume contained inside an EPP, reflecting its initial zipping angle (θ), plays a crucial role in actuation performance. When the air volume was low (small θ), the EPP fully zipped and generated high pressure, but higher air volume (large θ) caused reduction in electrostatic attractive force, partial zipping and decrease in pressure generation (Fig. 3b). The generated pressure increased with increasing applied voltage (Fig. 3c) as the attractive force and zipping were improved. The EPP requires only a small amount of liquid dielectric (18% of maximum available volume) to achieve its maximum performance (Fig. 3d), which significantly reduces the actuator weight, compared to other liquid-dielectric-amplified electrostatic actuators. When exploring different electrode dimensions, the EPP with a higher constrained zipping mechanism, caused by decreasing electrode width and increasing electrode thickness, generate higher pressure with a more effective parallel zipping motion. The EPP made of electrodes with $w = 3$ cm, $l = 4$ cm and $t = 0.1$ mm was capable of delivering the maximum pressure up to 12.24 kPa or the pressure difference (ΔP) of 11.25 kPa, which is 481% higher than the previous study[15] ($\Delta P = 2.34$ kPa). This generated pressure is higher than other electrostatic pneumatic pumps,[12,13] but less than a stretchable fluidic pump (14 kPa).[11]

A new design of the EPP pump was created by combining two identical zipping structures and minimising the inactive area. A soft foam was added to the centre of the pumps, acting as a compliant spring and providing a restoring force to return the pouch to its initial shape after zipping. This new design was able to produce similar instantaneous flow rate for different actuation frequencies (Fig. 6a), which corresponds to increasing averaged flow rate with increasing frequency (Fig. 6b). The pump was able to deliver a maximum averaged flow rate of 238 ml/min at 8 Hz actuation and at atmospheric pressure, which is 48% increase from the previous EPP design[15] (161 ml/min). The averaged flow rate at increasing pressure was also studied as illustrated in Fig. 6c. When comparing the actuator performance across different pump designs, different sizes of electrodes and foam resulted in different initial zipping angles (θ), and this θ is the major influence on the pressure and flow rate generated (Fig. 6d). When considering pumps made of the same electrodes but dissimilar θ, high flow rate was achieved by the pumps with large θ, whereas those with smaller θ produced higher pressures. In contrast, the pump with larger electrode size but similar θ was able to attain a higher flow rate since it contained a larger initial air volume to be transferred when actuated.

To improve the EPP pump further, a geometric design model is required to fabricate a scalable EPP with consistent effective zipping angle, maximising the electrostatic force induced between electrodes, ensuring flexural rigidity of the actuator structure, and optimising internal pressure and volume change. Replacing the soft foam

with a higher-response compliant spring could increase the flow rate while operating at higher frequencies since the pump could release rapidly ready for the next actuation cycle. Consequently, a small-scaled EPP can be created which produces high flow rate because only a very small zipping area is required at high frequencies. Moreover, separate air connectors could be explored (with new fabrication techniques) for the inlet (air suction) and outlet (pumping) so that they work independently to pump more efficiently at a high frequency.

ACKNOWLEDGMENTS

REFERENCES

[1] McCracken, J. M., Donovan, B. R., and White, T. J., "Materials as machines," *Advanced Materials* **32**(20), 1906564 (2020).

[2] Zhang, J., Sheng, J., O'Neill, C. T., Walsh, C. J., Wood, R. J., Ryu, J.-H., Desai, J. P., and Yip, M. C., "Robotic artificial muscles: Current progress and future perspectives," *IEEE transactions on robotics* **35**(3), 761–781 (2019).

[3] Bar-Cohen, Y. and Zhang, Q., "Electroactive polymer actuators and sensors," *MRS bulletin* **33**(3), 173–181 (2008).

[4] O'Halloran, A., O'malley, F., and McHugh, P., "A review on dielectric elastomer actuators, technology, applications, and challenges," *Journal of Applied Physics* **104**(7), 9 (2008).

[5] Guo, J., Leng, J., and Rossiter, J., "Electroadhesion technologies for robotics: A comprehensive review," *IEEE Transactions on Robotics* **36**(2), 313–327 (2019).

[6] Laser, D. J. and Santiago, J. G., "A review of micropumps," *Journal of micromechanics and microengineering* **14**(6), R35 (2004).

[7] Maffli, L., Rosset, S., and Shea, H., "Zipping dielectric elastomer actuators: characterization, design and modeling," *Smart Materials and Structures* **22**(10), 104013 (2013).

[8] Taghavi, M., Helps, T., and Rossiter, J., "Electro-ribbon actuators and electro-origami robots," *Science Robotics* **3**(25) (2018).

[9] Acome, E., Mitchell, S. K., Morrissey, T., Emmett, M., Benjamin, C., King, M., Radakovitz, M., and Keplinger, C., "Hydraulically amplified self-healing electrostatic actuators with muscle-like performance," *Science* **359**(6371), 61–65 (2018).

[10] Moretti, G., Duranti, M., Righi, M., Vertechy, R., and Fontana, M., "Analysis of dielectric fluid transducers," in [*Electroactive Polymer Actuators and Devices (EAPAD) XX*], **10594**, 142–154, SPIE (2018).

[11] Cacucciolo, V., Shintake, J., Kuwajima, Y., Maeda, S., Floreano, D., and Shea, H., "Stretchable pumps for soft machines," *Nature* **572**(7770), 516–519 (2019).

[12] Sîrbu, I., Moretti, G., Bortolotti, G., Bolignari, M., Diré, S., Fambri, L., Vertechy, R., and Fontana, M., "Electrostatic bellow muscle actuators and energy harvesters that stack up," *Science Robotics* **6**(51), eaaz5796 (2021).

[13] Cao, C., Gao, X., and Conn, A. T., "A magnetically coupled dielectric elastomer pump for soft robotics," *Advanced Materials Technologies* **4**(8), 1900128 (2019).

[14] Mao, G., Wu, L., Fu, Y., Chen, Z., Natani, S., Gou, Z., Ruan, X., and Qu, S., "Design and characterization of a soft dielectric elastomer peristaltic pump driven by electromechanical load," *IEEE/ASME Transactions on Mechatronics* **23**(5), 2132–2143 (2018).

[15] Diteesawat, R., Helps, T., Taghavi, M., and Rossiter, J., "Electro-pneumatic pumps for soft robotics," *Science Robotics* **6**(51) (2021).

[16] Suo, Z., "Theory of dielectric elastomers," *Acta Mechanica Solida Sinica* **23**(6), 549–578 (2010).

[17] Pohl, H. A., "The motion and precipitation of suspensoids in divergent electric fields," *Journal of applied Physics* **22**(7), 869–871 (1951).